Current leakage prevention in resistance welding of carbon fibre reinforced thermoplastics

Dubé, M.; Hubert, P.; Yousefpour, A.; Denault, J.

Publisher's version / Version de l'éditeur:
https://doi.org/10.1016/j.compscitech.2007.09.008
Composites Science and Technology, 68, 6, pp. 1579-1587, 2007-09-22

Available online at www.sciencedirect.com
ScienceDirect
Composites Science and Technology 68 (2008) 1579–1587
COMPOSITES SCIENCE AND TECHNOLOGY
www.elsevier.com/locate/compscitech

Current leakage prevention in resistance welding of carbon fibre reinforced thermoplastics

M. Dubé [a], P. Hubert [a,*], A. Yousefpour [b], J. Denault [c]

[a] McGill University, CREPEC, Department of Mechanical Engineering, 817 Sherbrooke Street West, Montréal, Québec, Canada H3A 2K6
[b] Aerospace Manufacturing Technology Centre, Institute for Aerospace Research, National Research Council Canada, 5145 Decelles Avenue, Montréal, Québec, Canada H3T 2B2
[c] Industrial Materials Institute, National Research Council Canada, 75 de Mortagne, Boucherville, Québec, Canada J4B 6Y4

Received 19 July 2007; received in revised form 11 September 2007; accepted 13 September 2007
Available online 22 September 2007

Abstract

Current leakage is a concern with resistance welding of carbon fibre reinforced thermoplastic composites. This phenomenon is particularly important when unidirectional adherends, with the carbon fibres parallel to the electrical current direction, are welded. In this investigation, a new electrically-insulated heating element consisting of a ceramic-coated (TiO_2) stainless steel mesh was developed to prevent current leakage. Special specimen geometry, called a skin/stringer configuration, was welded with this newly developed heating element to represent typical reinforced aerospace structures. The adherends were made of APC-2/AS4 (carbon fibre/PEEK) composites. Unidirectional specimens, which represent the most critical case, were first welded using the new heating element. The insulated heating element successfully prevented current leakage and showed great improvement in temperature homogeneity over the weld area. The impact of the new heating element on the mechanical performance of the welds was then assessed by welding quasi-isotropic specimens. The mechanical performances of quasi-isotropic specimens welded using the new insulated heating elements and conventional (non-insulated) ones were compared under short beam and three-point bending tests. No mechanical performance drawback was observed with the new heating element; however, the failure mode of the welded quasi-isotropic specimens was changed from a delamination in the skin laminate failure to a weld interface debonding failure.

Keywords: Resistance welding; A. Polymer–matrix composites (PMCs); A. Coating; E. Welding/joining; Current leakage

1. Introduction

Joining has been identified as one of the major issues in the implementation of continuous fibre reinforced composite structures in industry [1]. As the complexity of the components made of composite materials increases, efficient, reliable and low-cost joining methods are needed [2]. Conventional joining methods such as adhesive bonding and mechanical fastening have been developed for composite materials. In the case of thermoplastic–matrix composites, fusion bonding, or welding, is an advantageous joining method, as no extensive surface treatment is required and no stress concentrations are induced by the holes drilling process. Among the various available welding methods, resistance welding has been shown to be an efficient, simple and low-cost technique [3]. This welding process requires the application of a heating element between two thermoplastic composite parts to be welded (adherends). An electrical current is applied to the heating element and its temperature rises due to the Joule heating effect. As temperature rises, the surrounding polymer softens (amorphous polymers) or melts (semi-crystalline polymers). When the desired welding temperature is reached, the electrical current is stopped and the polymer cools down, under the application of pressure, resulting in a weld.

* Corresponding author. Tel.: +1 514 398 6303; fax: +1 514 398 7365.
E-mail address: pascal.hubert@mcgill.ca (P. Hubert).

0266-3538/$ - see front matter © 2007 Elsevier Ltd. All rights reserved.
doi:10.1016/j.compscitech.2007.09.008

The experimental studies performed on the resistance welding process shed light on some critical issues that need to be addressed before this technique can be fully implemented in industry [1,4–12]. Current leakage was expressed as a major concern when electrically conductive adherends, such carbon fibre reinforced thermoplastics, are welded [1,4,5,13]. When the polymer at the weld interface melts and flows, the heating element can get in contact with the carbon fibres of the adherends and as a result, new electrical paths are created in the adherends. Current leakage is an uncontrollable variable that results in long welding times, due to power losses in the adherends, and non-homogenous temperature distribution over the weld area. To remedy this problem, Don et al. [14] used two polymer films on each side of the heating element in order to prevent the heating element from touching the carbon fibres. This solution shows very limited success in preventing current leakage mostly because the melted polymer tends to squeeze out of the weld and thus no longer offers a barrier against current leakage. Another proposed solution was the use of a glass fibre ply on each side of the heating element [5,9]. This solution can successfully prevent the current leakage; however, it adds a foreign material in the weld, which reduces the weld strength and leads to a thicker specimen [9,13]. Another solution that was developed is spraying of a high-temperature resistive paint on the heating element [9]. The paint is electrically resistive and thermally stabile up to 600 °C. Good electrical insulation can be obtained with this method but the paint has to undergo a three-step curing cycle after it is applied on the heating element. This operation prolongs the resistance welding, which had the advantage of being a simple and fast technique. Current leakage thus remains an issue that needs to be addressed. So far, this problem has limited the applications of the resistance welding technique to glass fibre reinforced polymers.

In a previous study, resistance welding of a special specimen geometry, called a skin/stringer specimen, was investigated [15]. The specimens were made of a flange laminate, representing a stringer or frame, welded onto a skin laminate. This particular specimen geometry was selected as it represents a typical reinforced aerospace structure [16]. Both the flange and skin laminates were made of quasi-isotropic APC-2/AS4 (carbon fibre/PEEK) composite. The welding parameters, mechanical performance and failure modes of the specimens were investigated [15]. The present study uses the same skin/stringer geometry and pursues two main objectives: to develop a new insulated heating element that prevents current leakage and to analyse the effects of this insulated heating element on the mechanical performance and failure modes of the welded skin/stringer specimens.

2. Experimental procedures

2.1. Materials and specimen geometry

The adherends used in this study were made of 16 plies of unidirectional (UD) and quasi-isotropic $[\pm 45/90/0]_{2S}$ APC-2/AS4 composite laminates. The APC-2/AS4 laminates were provided by CYTEC Engineered Materials Inc. and were compression-moulded under a standard PEEK moulding condition, i.e., a processing temperature of 390 °C, a residence time of 20 min, a moulding pressure of 0.7 MPa and a cool down rate of approximately 7 °C/min. The laminates were 2.2 mm thick. In order to evaluate the efficiency of the current leakage solutions, specimens made of non-conductive material, which consisted of unidirectional 16 plies glass fibre/PEEK (GF/PEEK) adherends, were also welded, as a benchmark reference. The considered specimen geometry in all cases was the skin/stringer configuration with square-ended (non-tapered) flanges (Fig. 1) [15]. The skin laminate was 130 mm long and 25.4 mm wide and the flange was 50 mm long and 25.4 mm wide.

2.2. Resistance welding set-up

The resistance welding set-up consisted of a DC power supply with maximum output of 40 A and 80 V, a pressure system, a computer/data acquisition system and a resistance welding rig. The computer/data acquisition system was used to monitor the temperature, current and voltage in the welds. The current and voltage were monitored at the copper connectors. A control system was developed using National Instruments Labview software to control the input power. The control system was designed such a way that when temperature at the weld interface reached a pre-determined welding temperature of 440 °C, the electrical current was turned off [15].

The resistance welding rig that was used to weld the skin/stringer specimens was described in [17–19]. The heating element was placed between the skin and flange laminates. The ends of the heating element were clamped between the copper electrical connectors and the skin laminate (Fig. 2). A ceramic block was placed on the flange laminate to provide thermal insulation and facilitate a uniform pressure distribution on the weld surface. Two side ceramic blocks were used to prevent lateral movement of the flange during the welding process. All welds were conducted under a constant pressure of 1.0 MPa. Temperature during the welding operation was monitored using three

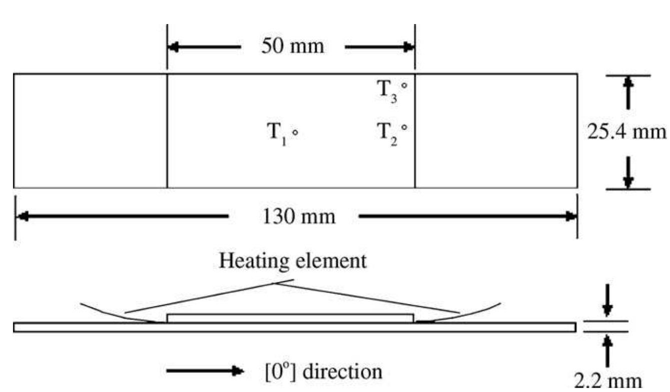

Fig. 1. Specimen geometry.

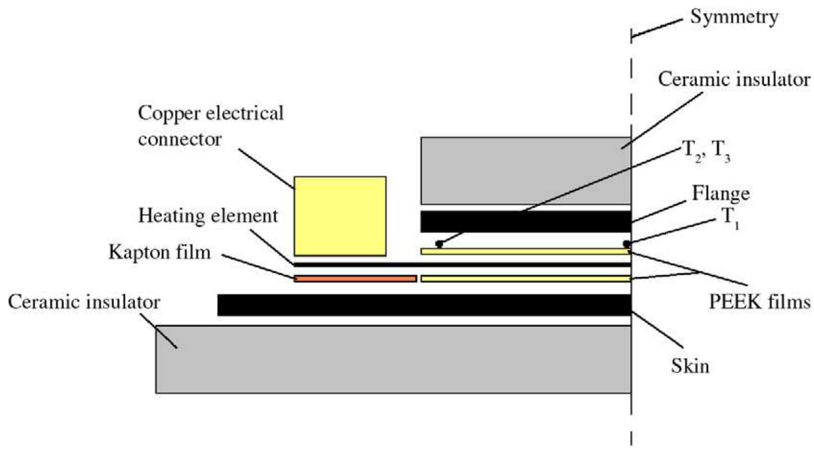

Fig. 2. Weld stack [15,17].

K-type thermocouples. One thermocouple was located at the centre of the weld (T_1), one was placed at the edge of the flange (T_2) and the last one was placed at the corner of the flange (T_3). All three thermocouples were positioned at the weld interface, between the top neat PEEK film and the flange laminate (Figs. 1 and 2).

The input power was applied to the heating element using the constant voltage method [11]. A constant voltage of 9.0 V was applied until the polymer reached the desired welding temperature of 440 °C. It is worth noting that, although the voltage was constant in this method, the input power varied. Since the electrical resistance of the stainless steel heating element increased with temperature, the input current, and thus the power, decreased accordingly. The monitored current and voltage data were used to calculate the electrical resistance according to the simple formula $R = V/I$ where R is the electrical resistance (Ω), V is the voltage (V) and I is the current (A). Plots of the electrical resistance as a function of the weld interface temperature were obtained from these data. Since the voltage was measured at the copper connectors' terminals, the calculated resistance was the summation of the copper connectors' resistances, the contact resistances between the heating element and connectors and the resistance of the heating element itself. All these resistances were considered to be in series. If current leakage occurred, then new electrical paths were created in the adherends and the new created electrical resistances were considered to be in parallel with the heating element resistance. In order to reduce the impact of the contact resistance between the connectors and heating element, a torque wrench was used to apply a clamping pressure of 16.3 MPa for each weld [5]. The contact resistance was constant since a constant clamping pressure was applied. Thus, the variations of electrical resistance were caused by the heating element or current leakage only.

2.3. Heating element preparation

The heating element was a stainless steel mesh with a wire diameter of 40 μm and an open gap width of 90 μm. The thickness of the mesh was 80 μm. A neat PEEK polymer film (thickness of 127 μm) was applied on each side of the mesh to provide a resin-rich region at the weld interface. This heating element, sandwich between these two polymer films, is referred to in the text as the conventional heating element (conventional HE). Two methods were elaborated to prevent current leakage to the adherends. The first method was similar to the one used by Don et al. [14] and consisted in applying a second polymer film to each side of the stainless steel mesh. That is, two films of a thickness of 127 μm were placed on each side of the mesh. This heating element is referred to as the two-films HE. The second insulation method was to coat the stainless steel mesh with a layer of nanostructured titanium oxide (TiO_2) powders. This powder was produced by Altair Nanomaterials Inc. and was deposited on the mesh using the high velocity oxy-fuel (HVOF) thermal spraying method. It was shown in a previous investigation that the nanostructured TiO_2 coating is tougher and more ductile than the conventional TiO_2 coating and provides a better interfacial bonding with the stainless steel substrates [20]. These characteristics explain the choice of the nanostructured TiO_2 coating for this investigation. The meshes were cut to the desired dimensions, cleaned with acetone and placed on an aluminium plate. HVOF spraying was then conducted on the meshes with special care not to coat the edges, which have to be connected to the copper electrical connectors. The TiO_2 layer applied on the heating element was 2 μm thick (Fig. 3). The TiO_2-coated heating elements are referred to as TiO_2 HE in the text.

2.4. Mechanical testing and characterisation methods

Short beam shear test was used to evaluate the interlaminar shear strength (ILSS) of the welded samples. These tests were carried out according to the ASTM D2344M standard test method. The samples were 4.6 mm thick and 9.0 mm wide. For the quasi-isotropic specimens, the samples were cut from the welded area according to Fig. 4a. In order to have the fibres in the length direction,

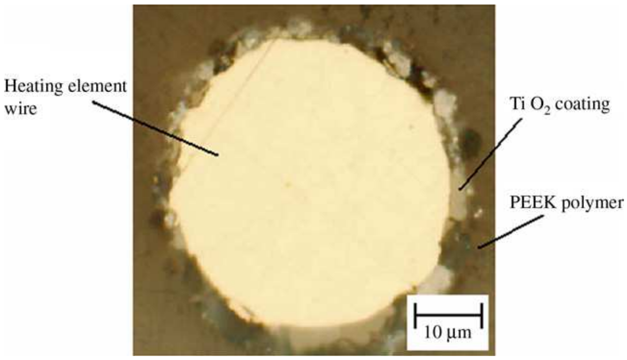

Fig. 3. TiO_2coating on a stainless steel wire.

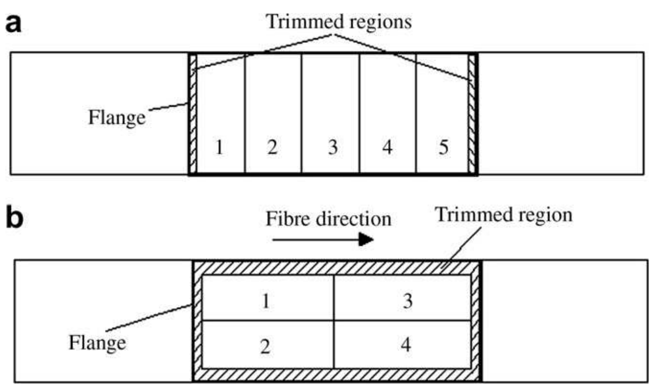

Fig. 4. Short beam samples of quasi-isotropic (a) and UD (b) specimens.

the samples of the UD specimens were cut as shown in Fig. 4b. A support span of 18 mm and a crosshead speed of 1.0 mm/min were used for all tests. For each welding condition, five replicated samples were tested for the quasi-isotropic specimens and four replicated samples were tested for the UD specimens. The ILSS were obtained from the first peak of the load–deflection curves. The fractured specimens were analysed by optical microscopy.

The mechanical performance of the welded skin/stringer configuration was evaluated using three-point bending tests. It was shown before that this test can represent the typical load case experienced by a reinforced aerospace structure, for example a fuselage, under the application of internal pressure [6,16]. A support span of 80 mm was used with a central load applied on the backside of the skin laminate. Specimens were tested at 23 °C and at relative humidity of 50% under a crosshead speed of 2.0 mm/min. The reported results are average of at least five replicated samples and the error bars correspond to two standard deviations. The various welding conditions and characterisation methods are summarised in Table 1.

3. Results and discussion

3.1. Electrical resistance

Current leakage can be detected through online monitoring the heating element electrical resistance during the welding process. Ageorges et al. [5] showed that when current leakage occurs, an electrical resistance drop is observed, due to the new electrical paths created in the adherends, mostly after the polymer melting temperature is reached. Fig. 5 presents the electrical resistance measured during welding of the UD and quasi-isotropic specimens as a function of the weld interface temperature. The standard deviation of the presented data is 5%. The electrical resistance of the GF/PEEK specimens, which did not allow any current leakage, is also shown for reference. As observed before by Don et al. [14], the two-films HE did not show any success in preventing current leakage. Initially, the electrical resistance increased with temperature (as expected for a stainless steel heating element) but started to decrease right after the PEEK melting temperature was reached. This reduction was due to melting of the polymer, which allowed the heating element mesh to come in contact with the carbon fibres of the adherends. New electrical paths were created in the adherends, reducing the overall electrical resistance of the system. Since the power supply was controlled by the voltage, the input electrical current kept increasing in order to match the reduced electrical resistance. When the power supply reached its maximum output current (40 A), it could no further maintain the constant targeted voltage. A reduction of voltage was then observed and the welding process was no longer controllable. Since it showed not much improvement in

Table 1
Welding conditions and characterisation methods

Welding conditions		Characterisation methods			
Adherend	Heating element	Electrical resistance monitoring	Temperature monitoring	Short beam shear test	Three-point bending test
UD APC-2/AS4	Conventional		×		
UD APC-2/AS4	Two films	×	×		
UD APC-2/AS4	TiO_2	×	×	×	×
UD GF/PEEK	Conventional	×	×		
Quasi-isotropic APC-2/AS4	Conventional	×	×	×	×
Quasi-isotropic APC-2/AS4	TiO_2	×	×	×	×

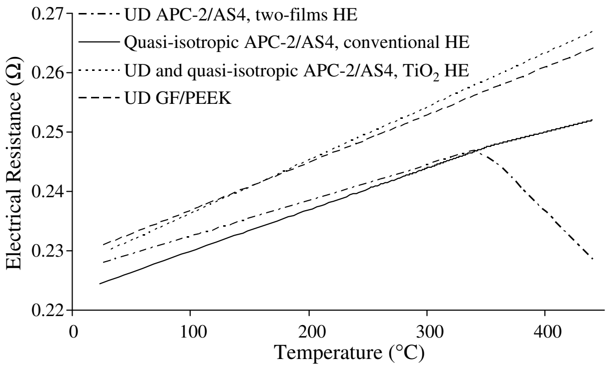

Fig. 5. Electrical resistance as a function of the weld interface temperature.

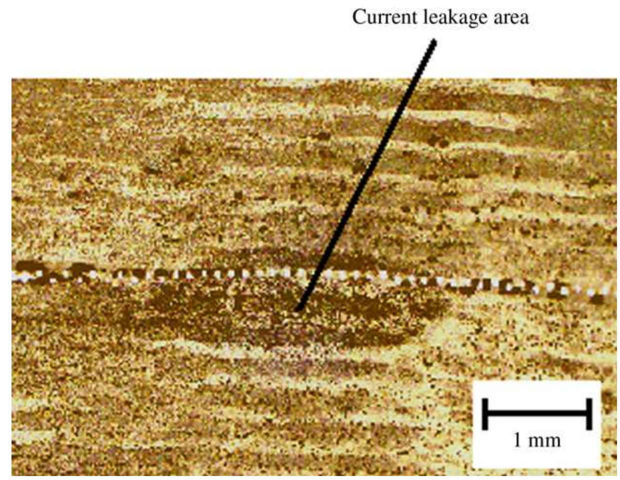

Fig. 6. Micrograph of the edge of a UD specimen welded using the two-films HE. The dark section represents the current leakage region, in which damaged fibres and polymer degradation were observed.

preventing current leakage, this two-films HE was no further investigated in this study.

In Fig. 5, it can also be observed that the specimens welded using the TiO_2 HE behaved as it is expected for a virgin stainless steel heating element, i.e., a constant electrical resistance increasing rate with temperature. No resistance drop was observed, showing the good electrical insulation provided by the TiO_2 coating. When comparing the APC-2/AS4 specimens welded using the TiO_2 HE with the GF/PEEK reference specimens, a 5% slope difference is observed. However, this slight difference was within the standard deviation of the measured data and was thus neglected. From the two attempted methods to reduce or eliminate current leakage in the UD specimens, the TiO_2 HE thus provided the best insulation.

In the case of the quasi-isotropic specimens, the 45° angle ply between the fibres next to the heating element and the electrical current direction increased the electrical resistance of the adherends, as no fibre was directly in contact with both ends of the heating element. Due to this 45° angle, it was expected that current leakage in the quasi-isotropic adherends would be reduced, even though no electrical insulation was used. However, some discrepancies were observed between these specimens and the GF/PEEK specimens or the ones welded using the TiO_2 HE. Fig. 5 shows that the slope of the quasi-isotropic specimens welded using the conventional HE started to decay after the PEEK melting temperature was reached. Current leakage, though reduced, was the reason for this behaviour. After the polymer melted, the combined effects of the stainless steel mesh (in which most of the current passed) and the carbon fibres of the adherends (in which an undetermined part of the current leaked) explained this lower slope. However, the controllability of the welding process was not affected due to the limited amount of current passing in the carbon fibres. As opposed to the UD specimens, it was still possible to weld the quasi-isotropic specimens with a good process control and accuracy, even without any electrical insulation.

The effect of current leakage was observed using optical microscopy. Dark areas existed at the edges of the UD specimens welded using the two-films HE, due to the damaged carbon fibres and polymer degradation in the first plies of the laminates. These dark areas were observed at both specimens ends, showing that current passed from one extremity of the specimens to the other, in the carbon fibres of the adherends (Fig. 6). These observations could be made only for the UD specimens. It was assumed that the reduced current leakage in the quasi-isotropic specimens did not damage the carbon fibres of the adherends nor induced polymer degradation, even when no electrical insulation was used.

3.2. Thermal behaviour

The UD specimens welded without insulation produced non-repeatable temperature profiles. Large temperature gradients and long welding times, caused by power losses in the adherends, were observed. Fig. 7 shows a comparison between the UD specimens welded with conventional and TiO_2 HE. It should be noted that due severe current leakage, it was hard to obtain consistent results for the specimens welded with the conventional HE. Therefore, the curve presented in Fig. 7a is a simple example of all the tests performed. The welding time without insulation was long and variable (130 s for the presented test) with non-uniform temperature distribution over the weld area, variable heating rate and temperatures up to 550 °C at the edges of the weld. The high temperatures reached at the edges of the welds led to polymer melting in these areas, which explained the fact that current leakage started right at the edges of the welds rather than in the middle (Fig. 6). In addition to these problems, many UD specimens could not be welded as current leakage prevented enough current from passing in the heating element. Fig. 7a shows that the large temperature gradients observed for the UD specimens initiated around the PEEK melting temperature of 343 °C, when the PEEK polymer melted and flowed, allowing the

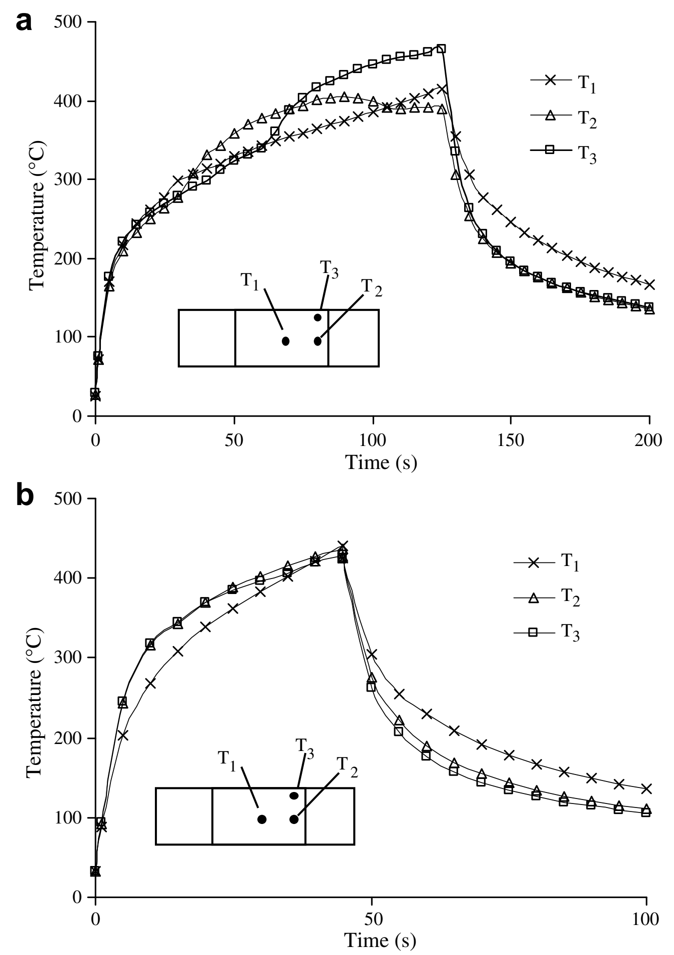

Fig. 7. Temperature profiles of UD APC-2/AS4 specimens welded using the conventional (a) and TiO_2 (b) HE.

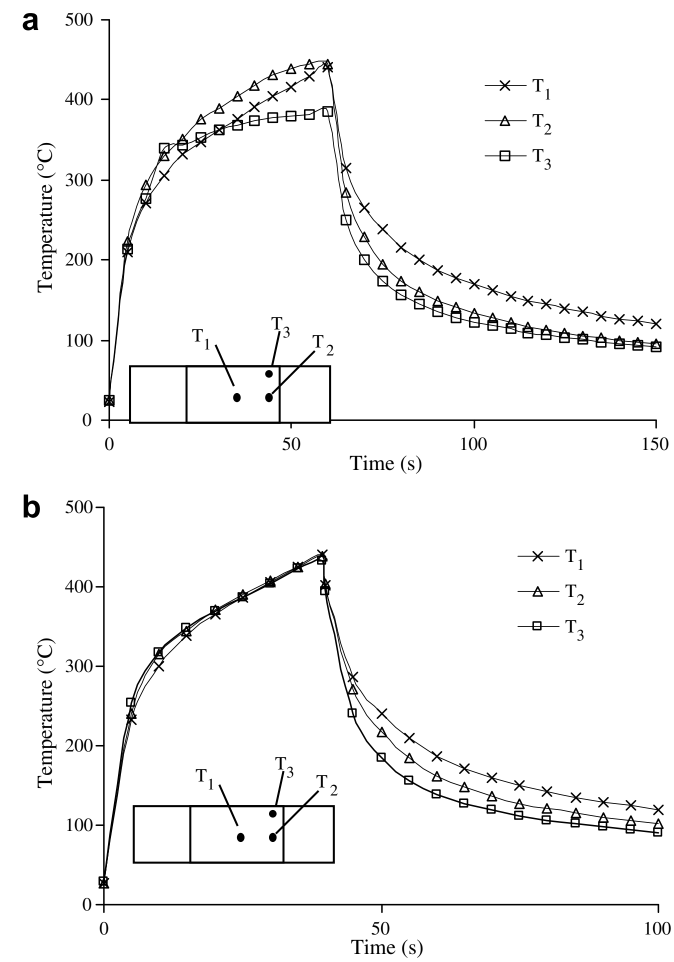

Fig. 8. Temperature profiles of quasi-isotropic APC-2/AS4 specimens welded using the conventional (a) and TiO_2 (b) HE.

heating element to touch the carbon fibres. The same type of curve was obtained with the two-films HE, showing, once again, the insufficient electrical insulation of this method. However, using the TiO_2 HE successfully prevented energy losses in the adherends and reduced the welding time from 130 s to 45 s. Temperature uniformity was also greatly improved with small temperature gradients (10 °C) between the edges and the centre of the welds. Since the TiO_2 coating was also applied on the exposed surfaces of the heating element, it acted as a thermal insulation on these areas, preventing the metal mesh from over-heating and thus, reducing the edge effect.

Fig. 8a shows the temperature profile of the quasi-isotropic specimens welded with the conventional HE. No major temperature gradient was observed after the polymer melted, as it was the case for the UD specimens welded using the conventional or two-films HE. The temperature gradient observed was simply due to the different thermal boundary conditions (edge effect). However, it was observed that the welding time of the quasi-isotropic specimens (60 s) was longer than the welding time of the UD specimens welded using the TiO_2 HE (45 s). The welding time of the quasi-isotropic specimens was reduced from 60 s to 40 s when using the TiO_2 HE (Fig. 8b). This confirmed the previous observations about current leakage in the quasi-isotropic adherends. Even though a larger electrical resistance existed in the adherends due to the 45° angle ply between the fibres next to the heating element and the electrical current direction, an undetermined part of the current leaked in the laminates. Using the TiO_2 HE reduced the welding time and provided better temperature homogeneity over the weld area. The temperature gradient between the edges and the centre was only 10 °C. As for the UD specimens, it was assumed that the TiO_2 coating on the exposed parts of the heating element acted as a thermal insulation and reduced the edge effect.

Fig. 9 presents the temperature profile of the GF/PEEK specimens. The welding time of these specimens was around 40 s, just as for the UD and quasi-isotropic specimens welded using the TiO_2 HE. This confirmed the excellent electrical insulation provided by the TiO_2 HE. It is also worth noting that the temperature vs. time curve of the GF/PEEK specimens showed the same non-uniform temperature as the quasi-isotropic APC-2/AS4 specimens welded using the conventional HE. Since no current leak-

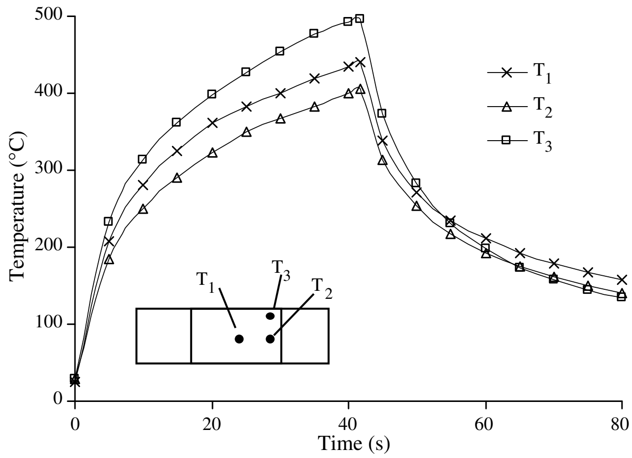

Fig. 9. Temperature profile of GF/PEEK specimens.

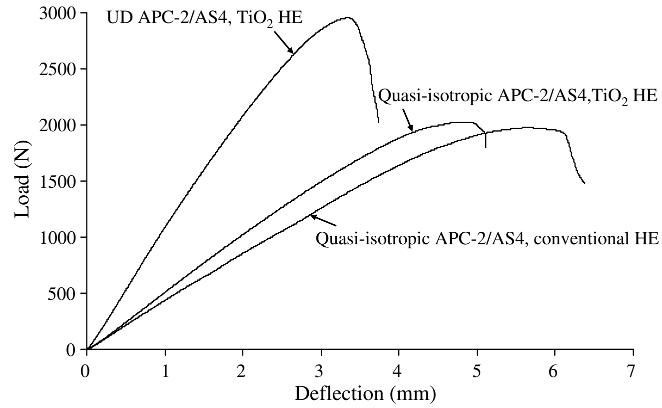

Fig. 11. Typical load–deflection curves under three-point bending.

age could be blamed for these temperature gradients, it was concluded that they were the result of the edge effect only.

3.3. Mechanical performance

The ILSS of the UD specimens welded using the TiO_2 HE and quasi-isotropic specimens welded using both the conventional and TiO_2 HE are presented in Fig. 10. The ILSS of the UD specimens was 99 N/mm^2 and the failure occurred at the weld interface. The ILSS of the quasi-isotropic specimens were 88 MPa and 94 MPa for the specimens welded using the conventional and TiO_2 HE, respectively. However, when considering the standard deviations, no difference is seen between the two results. In addition, in both cases the failure occurred in the laminates, at the 0° and 90° plies interface. As a reference, it was reported that the ILSS of the APC-2/AS4 quasi-isotropic laminates is 100 MPa [17].

The three-point bending tests results of the UD specimens (welded using the TiO_2 HE) and quasi-isotropic specimens (welded using the conventional and TiO_2 HE) are presented in Figs. 10 and 11. The maximum failure load of the UD specimens was 2814 N and the failure occurred at the weld interface. The first crack was located at the flange tip, between the skin laminate and the weld interface and then propagated in the weld, either between the skin laminate and the weld interface or in the weld itself, i.e., between the heating element wires and the TiO_2 coating. Comparison between the quasi-isotropic specimens welded using the conventional and TiO_2 HE revealed some discrepancies. Although the maximum failure loads were unchanged when considering the standard deviations, the load–deflection curves were different (Fig. 11). A rigidity increase of 20% was obtained for the TiO_2 HE, possibly due to the higher rigidity of the applied coating and its interfacial bond with the heating element. The failure modes were also different. As described in [15], the quasi-isotropic specimens welded using conventional HE showed a complex failure mode involving cracks at the weld interface and in the skin or flange laminates. However, when using the TiO_2 HE, the final failure of the specimens occurred in the weld itself, just as it was the case for the UD specimens. The first cracks were still located between the skin laminate and the weld interface, but the final delamination was in the weld, between the heating element wires and the TiO_2 coating. The fracture surfaces were observed under scanning electron microscopy to shade more light on the differences between the failure modes of the specimens welded using conventional and TiO_2 HE. For the specimens welded using conventional HE, no adherence was seen between the stainless steel wires and the PEEK polymer, due to low interfacial bonding between these two materials (Fig. 12a). The weld thus relied on mechanical interlocking between the polymer and the mesh. This lack of adherence between the stainless steel wires and the polymer was also observed for other polymers such as poly-ether-ketone-ketone (PEKK) and poly-ether-imide (PEI) [6]. However, the specimens welded using the TiO_2 HE exhibited adherence between the PEEK polymer and the TiO_2 coating. As seen in Fig. 12b, the coating had a rough surface, which facilitated adherence with the polymer. On the other hand, the TiO_2 coating tended to debond from the stainless steel wires. That is, good adherence was obtained between the coating and the polymer but not between the coating and

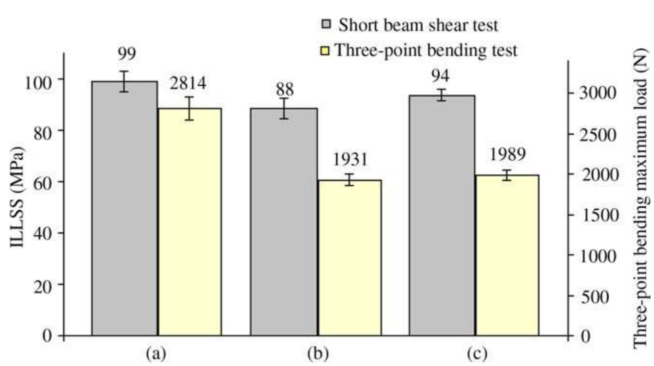

Fig. 10. Mechanical testing results of the UD specimens welded using the TiO_2 HE (a), quasi-isotropic specimens welded using conventional (b) and TiO_2 (c) HE.

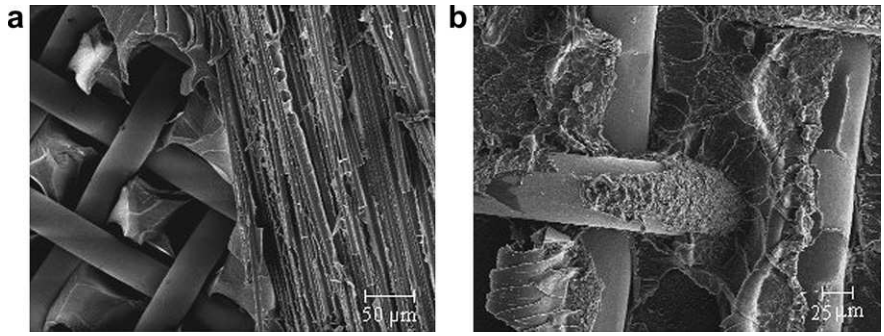

Fig. 12. Fracture surfaces of quasi-isotropic specimens welded using the conventional (a) [15] and TiO_2 (b) HE, under three-point bending.

the wires. However, as stated previously, this lack of adherence did not induce any mechanical performance penalty under the three-point bending tests, nor under the short beam shear tests.

4. Summary and conclusions

In this study, UD and quasi-isotropic APC-2/AS4 composite skin/stringer specimens were resistance-welded using a stainless steel mesh heating element. The electrical, thermal and mechanical behaviours of the welds were investigated. The mechanical performance was evaluated using short beam and three-point bending tests. Two methods were developed to prevent current leakage to the electrically conductive adherends and the following conclusions were drawn from the investigation:

(1) Current leakage to the electrically conductive adherends was found to be a major issue to weld the UD specimens. After the polymer at the weld interface was melted, an electrical resistance drop was observed, due to the new electrical current paths created in the adherends.
(2) The method consisting in applying two polymer films on each side of the heating element did not prevent current leakage. However, a new insulated heating element, consisting of a TiO_2-coated stainless steel mesh successfully prevented current leakage. No electrical resistance drop was observed when using this new method.
(3) The TiO_2 HE improved the temperature uniformity in the welds and reduced the welding time by preventing power losses in the adherends. The better temperature uniformity was attributed to the thermal insulation provided by the coating on the exposed parts of the heating element, which reduced the edge effect.
(4) The TiO_2 HE did not produce any mechanical performance drawback. The same ILSS was obtained as well as the same performance under three-point bending tests. However, the TiO_2 HE changed the failure mode of the quasi-isotropic specimens under three-point bending from delamination in the skin laminate to weld interface debonding.

Overall, the TiO_2 HE allowed the welding of UD specimens with good process control without affecting the static mechanical performance of the welds. However, the fatigue properties of the welds and the impact of the TiO_2 coating on the fatigue performance are still unknown. Since resistance welding finds applications in the aerospace industry, where parts are subjected to cyclic loadings, the fatigue behaviour of the welds should be the subject of future investigations.

Acknowledgements

This work was supported by funding from the Natural Sciences and Engineering Research Council of Canada. The authors also greatly acknowledge Cytec Engineered Materials Inc. for providing the materials used in this study, Dr. Rogerio Lima for technical advices concerning the TiO_2 deposition and Mr. Frédérick Belval for HVOF spraying.

References

[1] Eveno E, Gillespie JWJ. Resistance welding of graphite polyetheretherketone composites – an experimental investigation. J Thermoplast Compos Mater 1988;1:322–38.
[2] Silverman EM, Griese RA. Joining methods for graphite/PEEK thermoplastic composites. SAMPE J 1989;25(5):34–8.
[3] Stokes VK. Joining methods for plastics and plastic composites: an overview. Polym Eng Sci 1989;29(19):1310–24.
[4] Ageorges C, Ye L, Hou M. Experimental investigation of the resistance welding of thermoplastic–matrix composites. II. Optimum processing window and mechanical performance. Compos Sci Technol 2000;60(8):1191–202.
[5] Ageorges C, Ye L, Hou M. Experimental investigation of the resistance welding for thermoplastic–matrix composites. I. Heating element and heat transfer. Compos Sci Technol 2000;60(7):1027–39.
[6] Dubé M, Hubert P, Gallet JNAH, Stavrov D, Bersee HEN, Yousefpour A. Heating element optimization in resistance welding of semi-crystalline and amorphous thermoplastic composites. In: CANCOM, Winnipeg, Canada; 2007.
[7] Hou M, Friedrich K. Resistance welding of continuous carbon fibre/polypropylene composites. Plast Rubber Compos Process Appl 1992;18(4):205–13.
[8] Stavrov D, Bersee HEN. Thermal aspects in resistance welding of thermoplastic composites. In: ASME summer heat transfer conference, Las Vegas, USA; 2003.

[9] Stavrov D, Bersee HEN, Beukers A. Experimental investigation of large-scale welding of carbon fiber thermoplastic composite materials. In: International conference on composite materials, San Diego, USA; 2003.
[10] Stavrov D, Bersee HEN, Beukers A. The influence of the heating element on resistance welding of thermoplastic composite materials. In: International conference on composite materials, San Diego, USA; 2003.
[11] Yousefpour A, Simard M, Octeau M-A, Hojjati M. Process optimization of resistance-welded thermoplastic composites using metal mesh heating elements. In: SAMPE, Long Beach, USA; 2005.
[12] Yousefpour A, Simard M, Octeau M-A, Laramée M, Hojjati M. Effects of mesh size on resistance welding of thermoplastic composites using metal mesh heating elements. In: SAMPE-Europe, Paris, France; 2004.
[13] Stavrov D, Bersee HEN. Resistance welding of thermoplastic composites – an overview. Compos Part A: Appl Sci Manuf 2005;36(1):39–54.
[14] Don RC, Gillespie JW, Lambing CLT. Experimental characterisation of processing-performance relationships of resistance welded graphite/PEEK [polyetheretherketone] composite joints. Polym Eng Sci 1992;32(9):620–31.
[15] Dubé M, Hubert P, Yousefpour A, Denault J. Resistance welding of thermoplastic composites skin/stringer joints. Compos Part A: Appl Sci Manuf 2007. doi:10.1016/j.compositesa.2007.07.014.
[16] Minguet PJ, O'Brien TK. Analysis of test methods for characterizing skin/stringer debonding failures in reinforced composite panels. Composite materials: testing and design. In: Proceedings of the 12th symposium, Montréal, Canada; 1996.
[17] Dubé M, Hubert P, Yousefpour A, Denault J. Mechanical performance of resistance-welded thermoplastic composite skin/stringer specimen. In: SAMPE fall technical conference, Seattle, USA; 2005.
[18] Dubé M, Hubert P, Yousefpour A, Denault J. Fatigue performance of resistance-welded thermoplastic composite skin/stringer joints. In: SAMPE-Europe, Paris, France; 2007.
[19] Dubé M, Hubert P, Yousefpour A, Denault J, Wadham-Gagnon M. Resistance welding of thermoplastic composites skin/stringer specimens. In: SAMPE, Long Beach, USA; 2006.
[20] Lima BS, Marple BR. Enhanced ductility in thermally sprayed titania coating synthesized using a nanostructure feedstock. Mater Sci Eng A 2005;395:269–80.